



Short communication

## Temperature-controlled microwave solid-state synthesis of $\text{Li}_3\text{V}_2(\text{PO}_4)_3$ as cathode materials for lithium batteries

Gang Yang\*, Haidong Liu, Hongmei Ji, Zhongzhong Chen, Xuefan Jiang

Jiangsu Laboratory of Advanced Functional Material, Changshu Institute of Technology, Changshu 215500, China

## ARTICLE INFO

## Article history:

Received 10 October 2009

Received in revised form 31 January 2010

Accepted 9 March 2010

Available online 15 March 2010

## Keywords:

Lithium secondary batteries

Cathode material

Microwave solid-state synthesis

Electrochemistry

## ABSTRACT

Monoclinic  $\text{Li}_3\text{V}_2(\text{PO}_4)_3$  can be rapidly synthesized at  $750^\circ\text{C}$  for 5 min (MW5m) by using temperature-controlled microwave solid-state synthesis method (TCMS). The carbon-free sample MW5m presents well electrochemical properties. In the cut-off voltage 3.0–4.3, MW5m presents a charge capacity  $132\text{mAh g}^{-1}$ , almost equivalent to the reversible cycling of two lithium ions per  $\text{Li}_3\text{V}_2(\text{PO}_4)_3$  formula unit ( $133\text{mAh g}^{-1}$ ), and discharge capacity  $126.4\text{mAh g}^{-1}$ . In the cut-off voltage 3.0–4.8 V, MW5m shows an initial discharge capacity of  $183.4\text{mAh g}^{-1}$ , near to the theoretical discharge capacity. In the cycle performance, the capacity fade of  $\text{Li}_3\text{V}_2(\text{PO}_4)_3$  is dependent on the cut-off voltage and the preparation method.

© 2010 Elsevier B.V. All rights reserved.

### 1. Introduction

Rechargeable lithium-ion batteries are the most important power sources for the increasing demand from portable electronic products, electrical vehicles and hybrid electrical vehicles, etc. Commercial batteries utilize cobalt oxide as the positive electrode, but its high cost and toxicity prohibit the use in large-scale applications. Another class of cathode materials, transition-metal phosphates  $\text{LiMPO}_4$  ( $M = \text{Fe, Co, Ni, Mn}$ ) [1–3],  $\text{Li}_3\text{V}_2(\text{PO}_4)_3$  [4–6], and  $\text{LiVPO}_4\text{F}$  [7], have been proposed as the next generation cathode materials for lithium batteries because of their remarkable electrochemical performance and thermal stability. Among the above mentioned phosphates,  $\text{Li}_3\text{V}_2(\text{PO}_4)_3$  with both mobile  $\text{Li}^+$  cations and redox-active metal sites located within a rigid phosphate framework, has received intensive attention for the stable framework, higher operating voltage, and large theoretical capacity. Monoclinic lithium vanadium phosphate contains three independent lithium sites with a theoretical discharge capacity of  $197\text{mAh g}^{-1}$ , while three Li ions are completely extracted at the voltage of 4.8 V [4,5,8].

However, the low conductivity of  $\text{Li}_3\text{V}_2(\text{PO}_4)_3$  as  $\text{LiFePO}_4$  degrades its electrochemical performance. It is an effective method to improve the electrochemical performance by using carbon-coating process or the substitution of transition metal in vanadium site [9,10].  $\text{Li}_3\text{V}_2(\text{PO}_4)_3$  had already been prepared by using hydrogen or carbon as reduction agents [5,11]. These synthesis

processes need high calcinations temperature and long reaction time.

There are many synthesis methods applied to cathode materials, including conventional solid-state synthesis, hydrothermal, and sol-gel etc. The microstructure and property of the materials are always dependent on the synthesis methods. Over the past decade, microwave heating has become an important method in chemical synthesis and materials processing. Since the microwave energy is directly absorbed by the sample, uniform and rapid heating can be achieved within several minutes. Microwave solid-state synthesis method has already been applied to synthesize a number of inorganic materials, such as carbides, nitrides, complex oxides, silicides, and zeolites, etc. [12–19]. Microwave solid-state synthesis method as a novel method has been developed to prepare cathode materials for lithium batteries [12–15,19]. In our previous paper, the heating behavior and crystal growth mechanism of  $\text{LiV}_3\text{O}_8$  have been reported. The structure, morphology and the electrochemical performance of  $\text{LiV}_3\text{O}_8$  have been found that it is dependent on the microwave irradiation condition [14]. The microwave synthesis of solid-state materials in lab is mostly done with domestic microwave oven which are inexpensive and convenient. However, several limitations appeared in the solid-state synthesis by using domestic microwave oven. First, because the traditional metal thermocouple is not suitable used in microwave field, the reaction temperature was unknown and cannot be controlled in domestic microwave oven; second, without a well-insulated material the domestic microwave oven cannot stand the high reaction temperature (more than  $600^\circ\text{C}$ ) needed in the solid-state preparation of inorganic material; third, the reaction atmosphere cannot be controlled. For example, Higuchi et al. [12] reported the preparation of

\* Corresponding author. Tel.: +86 512 52251898; fax: +86 512 52251842.

E-mail addresses: [gyang@csit.edu.cn](mailto:gyang@csit.edu.cn), [yanggang9989@yahoo.com.cn](mailto:yanggang9989@yahoo.com.cn) (G. Yang).

LiFePO<sub>4</sub> by using domestic microwave oven. In their reaction system, the reactants pellet was covered with glass wool to insulate the high reaction temperature avoiding the damage of microwave oven. Moreover, in addition to the product LiFePO<sub>4</sub>, impurity phase of Li<sub>3</sub>Fe<sub>2</sub>(PO<sub>4</sub>)<sub>3</sub> was produced due to the domestic microwave cannot assure the reaction in an well inert atmosphere.

In this paper, the carbon free Li<sub>3</sub>V<sub>2</sub>(PO<sub>4</sub>)<sub>3</sub> has been synthesized in 5 min by using temperature-controlled microwave solid-state synthesis tube furnace. Because the surface temperature of the sample pellet directly detected by an infrared pyrometer, the microwave irradiation power and the reaction temperature are automatically controlled by a computer. The lattice parameter of the rapidly formed Li<sub>3</sub>V<sub>2</sub>(PO<sub>4</sub>)<sub>3</sub> is refined, and the electrochemical properties are discussed in detail.

## 2. Experimental

Li<sub>3</sub>V<sub>2</sub>(PO<sub>4</sub>)<sub>3</sub> is synthesized using V<sub>2</sub>O<sub>5</sub>, NH<sub>4</sub>H<sub>2</sub>PO<sub>4</sub>, Li<sub>2</sub>CO<sub>3</sub>, and H<sub>2</sub>C<sub>2</sub>O<sub>4</sub> in stoichiometric. H<sub>2</sub>C<sub>2</sub>O<sub>4</sub> is used here as chelating agent and reducing agent. H<sub>2</sub>C<sub>2</sub>O<sub>4</sub> and V<sub>2</sub>O<sub>5</sub> are absolutely reacted to form a clear solution, and a mixture of NH<sub>4</sub>H<sub>2</sub>PO<sub>4</sub> and Li<sub>2</sub>CO<sub>3</sub> is added to form a gel at 70 °C. The gel decomposed at 350 °C in argon atmosphere for 4 h. The obtained precursor is grounded and pressed into two pellets under the pressure of 5 MPa. One pellet is synthesized in a convention furnace, at 750 °C for 10 h in argon (named as CP10h). The other pellet is irradiated at 750 °C for 5 min in argon by using microwave solid-state synthesis tube furnace (named as MW5m). The temperature-controlled microwave solid-state synthesis tube furnace is a multimode oven with an adjustable power output (Frequency 2.45 GHz, Maximum power 2 kW). A water-cooled multimode cavity consists of a quartz tube ensuring a controlled atmosphere. Because the surface temperature of the sample pellet is directly detected by an infrared pyrometer (Raytek, Marathon series), the microwave irradiation power and the reaction temperature are automatically controlled by a computer. The accuracy of temperature recorded by this system is generally within ±1 °C over the whole range of heating. About 3 g reactants pellet place in the center of an alumina tube, and the alumina tube is placed inside a well-insulated kaowool canula.

X-ray studies are done on a Rigaku diffractometer with Cu K $\alpha$  radiation. The diffraction data are collected for 4 s at each 0.02° step width. The lattice parameters of Li<sub>3</sub>V<sub>2</sub>(PO<sub>4</sub>)<sub>3</sub> are refined by Rietveld analysis using the General Structure Analysis System (GSAS) [20].

Electrochemical performance of samples is evaluated in CR2016 coin cells at 25 °C. Li<sub>3</sub>V<sub>2</sub>(PO<sub>4</sub>)<sub>3</sub> is mixed with acetylene black and Teflon powder in the weight ratio 80:15:5. Lithium foil is used as the anode, 1 M LiPF<sub>6</sub> in EC: DMC = 1:1 as the electrolyte, Celgard 2300 membrane as separator. Cyclic voltammetry (CV) are conducted on PARSTAT2273 electrochemical workstation at scan rate 0.2 mV s<sup>-1</sup>. Charge–discharge performances are carried out on Land CT2001A at 0.1 C. The cut-off voltages are 3.0–4.3 V and 3.0–4.8 V, respectively.

## 3. Results and discussion

Chemical synthesis by microwave heating is very efficient, since it offers rapid volumetric heating and high reaction rates. In the temperature-controlled microwave solid-state synthesis process (TCMS), the homogeneous effects induced by microwave irradiation could create a uniform nucleation condition.

XRD pattern refinements of the samples Li<sub>3</sub>V<sub>2</sub>(PO<sub>4</sub>)<sub>3</sub> synthesized under conventional and microwave solid-state synthesis are shown in Fig. 1. All X-ray diffraction peaks correspond to a single-

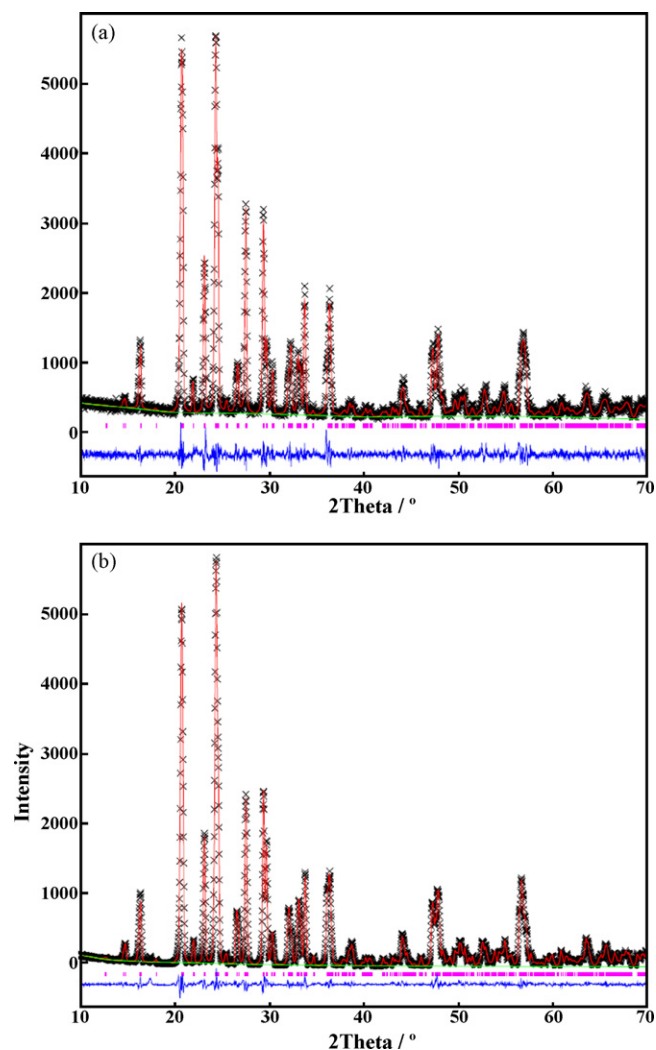


**Fig. 1.** Observed (×) and calculated (solid line) XRD patterns for Li<sub>3</sub>V<sub>2</sub>(PO<sub>4</sub>)<sub>3</sub> samples synthesized by (a) conventional solid-state synthesis at 750 °C for 10 h, and (b) microwave solid-state synthesis at 750 °C for 5 min. The difference between the observed and the calculated data is given at the bottom of the figure with the same scale. Peak positions of Li<sub>3</sub>V<sub>2</sub>(PO<sub>4</sub>)<sub>3</sub> phase are expressed as vertical lines.

phase, and can be indexed as monoclinic structure with a space group of P2<sub>1</sub>/n. By comparison with the relatively long reaction time (about dozen hours) of Li<sub>3</sub>V<sub>2</sub>(PO<sub>4</sub>)<sub>3</sub> formed in conventional solid-state synthesis method, these experimental facts confirm that the crystal growth of Li<sub>3</sub>V<sub>2</sub>(PO<sub>4</sub>)<sub>3</sub> lattice could be dramatically accelerated under microwave irradiation field. The lattice structure of MW5m will be affected due to the fast crystal formation.

The refined lattice parameters and atomic coordination of MW5m and CP10h are listed in Table 1. Because the reliability factor of  $\chi^2$  is less than 3, and the weighted factor  $R_{wp}$ ,  $R_f$  and  $R_p$  less than 10% (listed at the bottom of Table 1), the Rietveld refinement results are reliable in the following analysis of crystal structure. All the Li, V, P, and O atoms occupy Wyckoff position 4e. Three lithium ions reside in one tetrahedral site and two pseudotetrahedral sites [5,10]. The main difference appeared in lattice constants and atomic fractional coordinates is the three mobile lithium ions of Li<sub>3</sub>V<sub>2</sub>(PO<sub>4</sub>)<sub>3</sub> synthesized by conventional solid-state synthesis and TCMS, respectively. For example, the fractional coordinates of Li1(4e) of MW5m are 0.3502(2), 0.3350(1), and 0.2995(2)Å, compared with 0.2971(1), 0.2722(8), and 0.4875(1)Å

**Table 1**  
Atomic sites and fractional coordinates of  $\text{Li}_3\text{V}_2(\text{PO}_4)_3$ .

Atom	x		y		z	
	CP10h <sup>a</sup>	MW5m <sup>b</sup>	CP10h	MW5m	CP10h	MW5m
Li1(4e)	0.2971(1)	0.3502(2)	0.2722(8)	0.3350(1)	0.4875(1)	0.2995(2)
Li2(4e)	0.6277(3)	0.5638(3)	0.2657(2)	0.1941(2)	0.1329(3)	0.4135(3)
Li3(4e)	0.9214(0)	0.9431(2)	0.2856(3)	0.2474(2)	0.3014(0)	0.3300(2)
V1(4e)	0.2475(9)	0.2479(4)	0.1111(4)	0.1105(2)	0.4681(5)	0.4619(6)
V2(4e)	0.7514(9)	0.7496(4)	0.3890(4)	0.3900(8)	0.4672(5)	0.4685(6)
P1(4e)	0.1047(2)	0.1046(5)	0.1520(1)	0.1507(7)	0.1030(1)	0.1040(6)
P2(4e)	0.5995(1)	0.6094(6)	0.3590(8)	0.3527(4)	0.1148(1)	0.1149(6)
P3(4e)	0.0300(1)	0.0365(5)	0.5087(1)	0.4932(4)	0.2453(1)	0.2541(7)
O1(4e)	0.4462(2)	0.4430(1)	0.3472(2)	0.3359(6)	0.1177(2)	0.0792(1)
O2(4e)	0.9376(2)	0.9287(1)	0.1485(2)	0.1447(6)	0.0927(2)	0.1176(9)
O3(4e)	0.6054(0)	0.3553(1)	0.1393(3)	0.2667(7)	0.5119(3)	0.4762(1)
O4(4e)	0.8238(2)	0.8083(8)	0.2043(1)	0.2199(6)	0.3909(2)	0.4922(9)
O5(4e)	0.1814(2)	0.1741(1)	0.0344(9)	0.0485(7)	0.0410(1)	0.0545(1)
O6(4e)	0.6395(2)	0.6578(1)	0.4742(2)	0.4721(6)	0.0890(2)	0.0842(9)
O7(4e)	0.4516(2)	0.4570(1)	0.0648(1)	0.0697(7)	0.3780(2)	0.3713(1)
O8(4e)	0.9632(2)	0.9257(9)	0.3949(2)	0.4046(6)	0.3155(2)	0.3311(8)
O9(4e)	0.1451(1)	0.1635(1)	0.4374(8)	0.4318(6)	0.1842(1)	0.1669(1)
O10(4e)	0.6468(2)	0.6164(9)	0.0825(2)	0.0774(5)	0.1698(2)	0.1278(1)
O11(4e)	0.2089(2)	0.1642(9)	0.1535(1)	0.1767(6)	0.2406(2)	0.2511(1)
O12(4e)	0.6635(2)	0.6363(9)	0.3198(2)	0.3232(7)	0.2765(2)	0.2908(1)

<sup>a</sup> For the sample CP10h, lattice constants  $a = 8.5905(1)\text{\AA}$ ,  $b = 12.0352(25)\text{\AA}$ ,  $c = 8.6171(4)\text{\AA}$  and  $\beta = 90.3801(0)^\circ$ , the reliable factors are  $R_{\text{wp}} = 11.68\%$ ,  $R_p = 8.72\%$ ,  $\chi^2 = 1.631$ , and  $R_f = 5.03\%$ .

<sup>b</sup> For the sample MW5m, lattice constants  $a = 8.6059(9)\text{\AA}$ ,  $b = 12.0359(5)\text{\AA}$ ,  $c = 8.5942(2)\text{\AA}$  and  $\beta = 90.5779(2)^\circ$ , the reliable factors are  $R_{\text{wp}} = 6.60\%$ ,  $R_p = 4.53\%$ ,  $\chi^2 = 1.239$ , and  $R_f = 3.14\%$ .

of  $\text{Li}_3\text{V}_2(\text{PO}_4)_3$  synthesized at  $750^\circ\text{C}$  for 10 h. The deviation in atomic coordination is attributed to the strain in the crystal structure as a result of high tension and the mismatching coefficient diffusion of lithium ions with the formation of rigid framework by  $\text{VO}_6$  and  $\text{PO}_4$  polyhedra because of the too fast crystal growth process.

The powder characters are verified through SEM and TEM observation analysis. The SEM and TEM micrographs of the samples MW5 and CP10h are shown in Fig. 2. Because of the rapid heating behavior,  $\text{Li}_3\text{V}_2(\text{PO}_4)_3$  (MW5m) could be synthesized at 5 min compared with the dozens of hours needed in traditional solid-state

synthesis method (CP10h). The sample MW5m presents relatively lower crystallinity and small crystallites (about 100 nm). However, relatively higher crystallinity and bigger crystal size (about  $1\ \mu\text{m}$ ) are presented in Fig. 2b and b' due to the long reaction time.

Several published reports described that  $\text{Li}_3\text{V}_2(\text{PO}_4)_3$  samples need carbon coating for good electrochemical performance [9,10]. In this manuscript, the carbon-free MW5m sample synthesized by TCMS presents well electrochemical properties. Cyclic voltammetry recorded for MW5m is shown in Fig. 3. There are three couples of oxidation and reduction peaks between 3.0 and 4.5 V (as shown

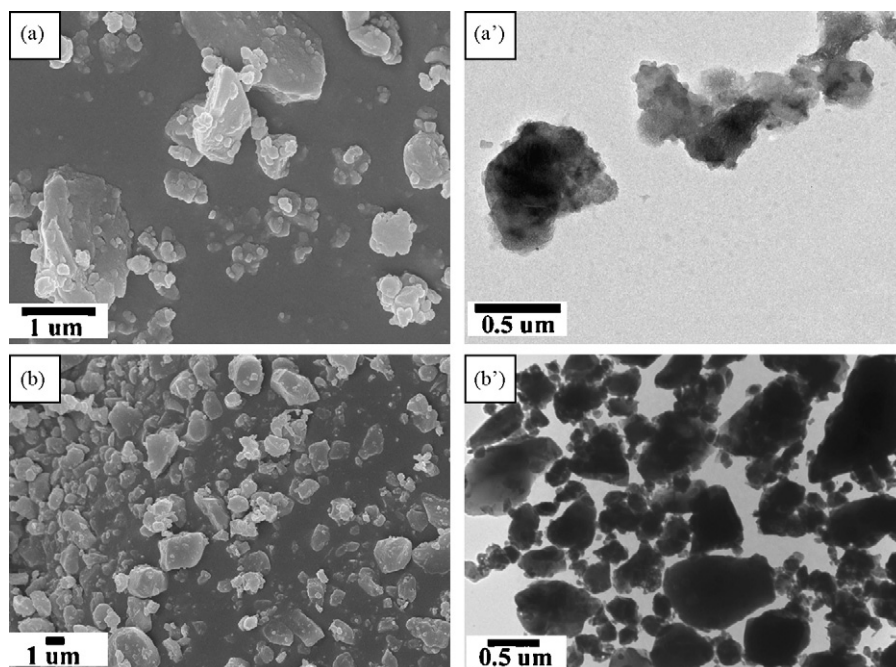


**Fig. 2.** SEM and TEM images of  $\text{Li}_3\text{V}_2(\text{PO}_4)_3$  samples (a) and (a') MW5m, and (b) and (b') CP10h.

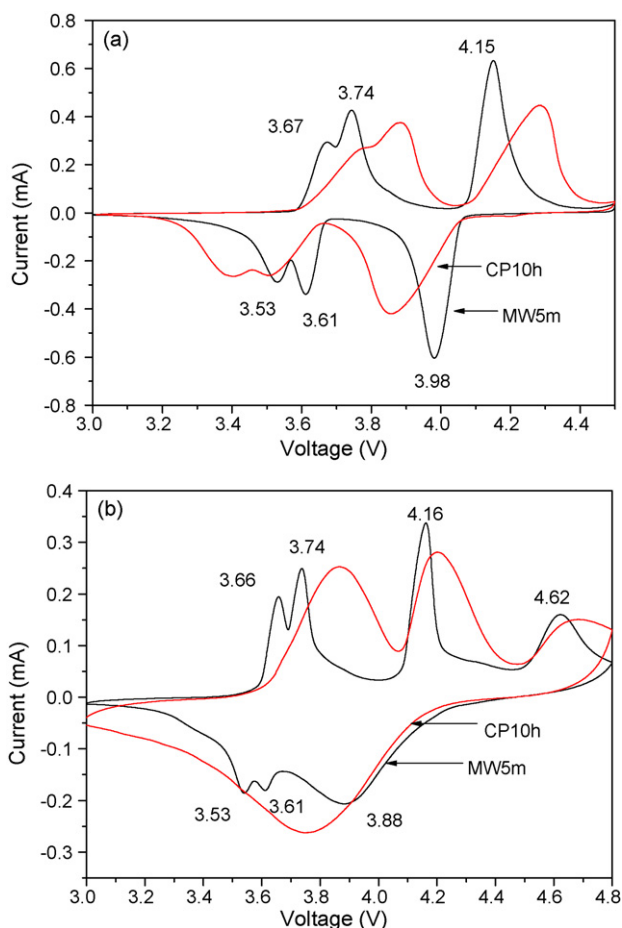


**Fig. 3.** Cyclic voltammetry of MW5m and CP10h for initial cycle at the voltage range from (a) 3.0 to 4.5 V, and (b) 3.0 to 4.8 V.

in Fig. 3a). The two oxidation peaks around 3.67 and 3.74 V correspond to the removal of the first  $\text{Li}^+$  in two steps, because there is an ordered  $\text{Li}_{2.5}\text{V}_2(\text{PO}_4)_3$  phase [5,8]. The second  $\text{Li}^+$  ion is extracted through one single step around 4.15 V. During the anodic process, the three peaks located at 3.53, 3.61 and 3.98 V can be attributed to the reinsertion of the two  $\text{Li}^+$  ions, associate with the  $\text{V}^{4+}/\text{V}^{3+}$  redox couples. The well-defined peaks and smaller value of potential interval shows the good reaction reversibility of MW5m. To investigate the extraction/insertion process of the third lithium ion in  $\text{Li}_3\text{V}_2(\text{PO}_4)_3$ , the CV profile of MW5m in the voltage range 3.0–4.8 V presents four oxidation and three reduction peaks present in the CV curve (as shown in Fig. 3b). The oxidation peak at 4.62 V is the extraction of the third  $\text{Li}^+$  ion, associated with the phase transition process from  $\text{LiV}_2(\text{PO}_4)_3$  to  $\text{V}_2(\text{PO}_4)_3$ . However, there is the absent of the corresponding reduction peak in the CV curves. It is agree with the previous results that the initial reinsertion of  $\text{Li}^+$  cation in  $\text{V}_2(\text{PO}_4)_3$  from a solid solution of two phase [5]. By comparison, there is a relatively bigger value of potential interval in the redox process of CP10h. For example, the CV plot of CP10h shows a wide reduction peak between 3.0 and 4.8 V (as shown in Fig. 3b). It might be due to the fact that the big crystal size of CP10h limits the extraction/reinsertion ability of Li cations. The similar results would be concluded in the followed charge/discharge analysis of  $\text{Li}_3\text{V}_2(\text{PO}_4)_3$ .

Fig. 4 shows the initial and 30th charge–discharge profiles of the MW5m and CP10h electrode at 0.1 C ( $13.3 \text{ mA g}^{-1}$ ) in the voltages of 3.0–4.3 V. The carbon-free sample MW5m shows specific charge capacity  $132.0 \text{ mAh g}^{-1}$ , almost equivalent to the reversible

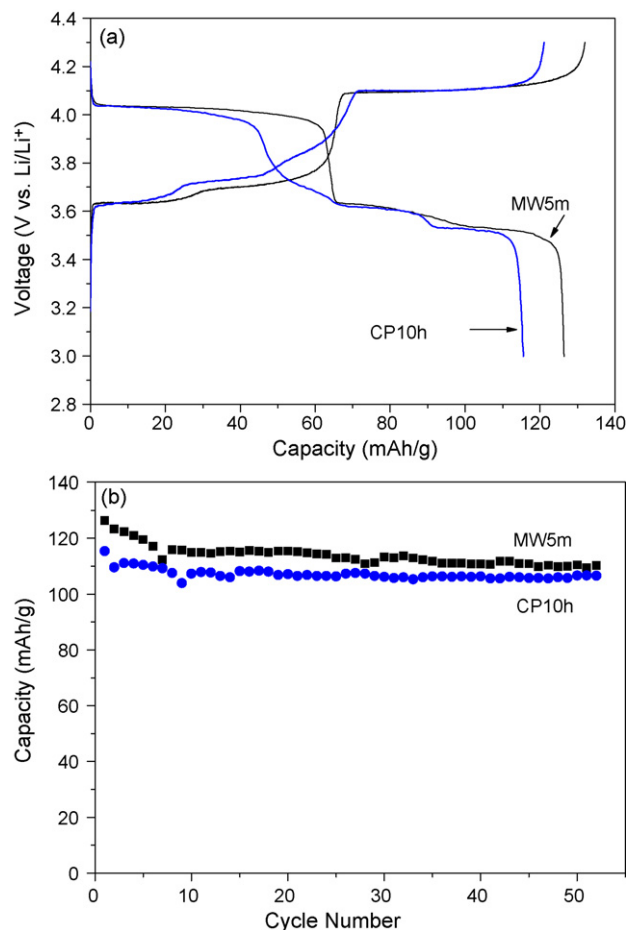


**Fig. 4.** (a) Initial charge/discharge profiles and (b) cyclic performance of  $\text{Li}_3\text{V}_2(\text{PO}_4)_3$  in the voltage range of 3.0–4.3 V.

cycling of two lithium ions per  $\text{Li}_3\text{V}_2(\text{PO}_4)_3$  formula unit. The specific discharge capacity of MW5m is  $126.4 \text{ mAh g}^{-1}$ . The electrode of carbon-free sample CP10h exhibits a reversible specific charge and discharge capacity of 121.1 and  $115.5 \text{ mAh g}^{-1}$ , respectively. Three couples of charge/discharge plateaus at 4.09/4.03 V, 3.70/3.64 V and 3.63/3.56 V, corresponded to three compositional regions of  $\text{Li}_{3-x}\text{V}_2(\text{PO}_4)_3$  ( $x=0-0.5$ ,  $x=0.5-1.0$  and  $x=1.0-2.0$ ), respectively.

As shown in Fig. 5, the rapidly synthesized sample MW5m by TCMS presents an initial charge capacity of  $197 \text{ mAh g}^{-1}$ , equivalent to the reversible cycling of three lithium ions per  $\text{Li}_3\text{V}_2(\text{PO}_4)_3$  formula unit ( $197 \text{ mAh g}^{-1}$ ). The initial specific discharge capacity of MW5m is  $183.4 \text{ mAh g}^{-1}$ . The  $\text{Li}_3\text{V}_2(\text{PO}_4)_3$  sample CP10h presents an initial charge and discharge capacity 156.1 and  $144.9 \text{ mAh g}^{-1}$ , respectively. This indicates that the rapidly formed crystal structure has significant contribution to the improvement on the electrochemical performance. After dozens cycles of charge and discharge, the above two samples present a significantly capacity fade (as shown in Fig. 5b), compared with the good cycleability presented in the cut-off voltage 3.0–4.3 V (Fig. 4b). For example, after 50th cycle the discharge specific capacity of MW5m remains  $123.7 \text{ mAh g}^{-1}$ , and that of CP10h is only  $57.3 \text{ mAh g}^{-1}$  after 10 cycles.

The detailed crystal growth mechanism of  $\text{Li}_3\text{V}_2(\text{PO}_4)_3$  and the relative electrochemical properties of  $\text{Li}_3\text{V}_2(\text{PO}_4)_3$  synthesized under different microwave irradiation condition would be discussed in the following paper.

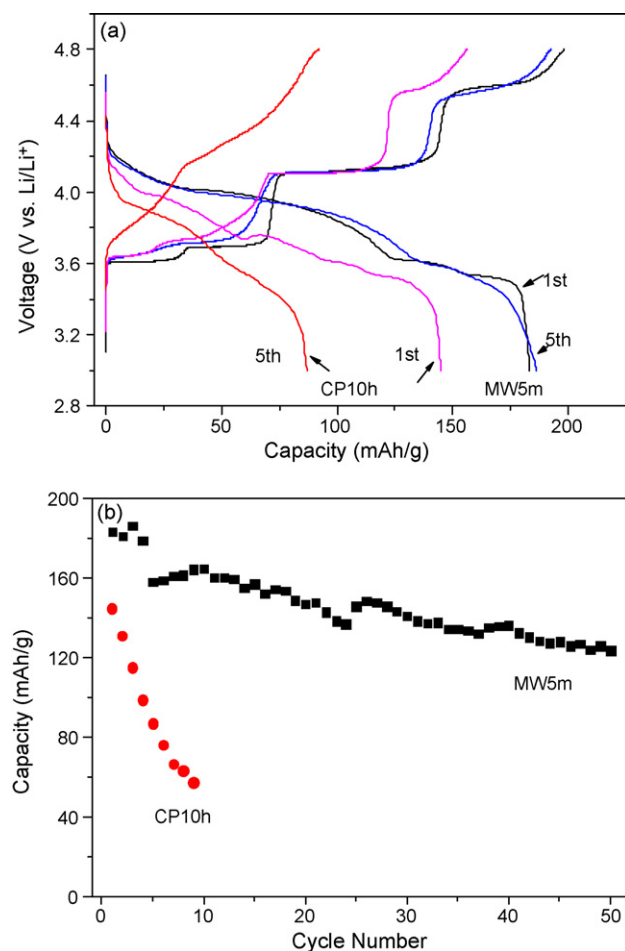


Fig. 5. (a) Charge/discharge profiles and (b) cyclic performance of  $\text{Li}_3\text{V}_2(\text{PO}_4)_3$  in the voltage range of 3.0–4.8 V.

#### 4. Conclusions

Monoclinic  $\text{Li}_3\text{V}_2(\text{PO}_4)_3$  is rapidly synthesized at 750 °C for 5 min by TCMS. The crystal growth of  $\text{Li}_3\text{V}_2(\text{PO}_4)_3$  lattice is dramatically accelerated in microwave irradiation field. Because of the too fast crystal growth process, the refined cell parameters and atomic coordination of MW5m shows some deviation, especially  $\text{Li}^+$  coordination. The sample MW5m presents relatively lower crystallinity and small crystallites (about 100 nm) compared with the relatively higher crystallinity and bigger crystal size (about 1  $\mu\text{m}$ )

presented in CP10h due to the long reaction time. A well-defined peaks and smaller value of potential interval shows the good redox process in MW5m. In the cut-off voltage 3.0–4.8 V, the rapidly synthesized sample MW5m presents an initial charge capacity of 197  $\text{mAh g}^{-1}$ , equivalent to the reversible cycling of three lithium ions per  $\text{Li}_3\text{V}_2(\text{PO}_4)_3$  formula unit. The initial discharge capacity of MW5m is 183.4  $\text{mAh g}^{-1}$ . However, compared with the good cycleability presented in the cut-off voltage 3.0–4.3 V, carbon-free  $\text{Li}_3\text{V}_2(\text{PO}_4)_3$  presents a significant capacity loss in the cut-off voltage 3.0–4.8 V. The capacity fade of  $\text{Li}_3\text{V}_2(\text{PO}_4)_3$  is dependent on the cut-off voltage and the preparation method, more capacity lost at relatively higher charge/discharge voltage.

#### Acknowledgments

The authors acknowledge the supports of Natural Science Foundation of Jiangsu Province of China (BK2006537), Natural Science Foundation of Jiangsu Educational Department of China (06KJA43014), and Natural Science Foundation of China (10874021).

#### References

- [1] A.K. Padhi, K.S. Nanjundaswamy, J.B. Goodenough, *J. Electrochem. Soc.* 144 (1997) 1188.
- [2] B. Kang, G. Ceder, *Nature* 458 (2009) 190.
- [3] C. Delmas, M. Maccario, L. Croguennec, F. Le-Cras, F. Weill, *Nat. Mater.* 7 (2008) 665.
- [4] H. Huang, S.C. Yin, T. Kerr, N. Taylor, L.F. Nazar, *Adv. Mater.* 14 (2002) 1525.
- [5] S.C. Yin, H. Grondey, P. Strobel, M. Anne, L.F. Nazar, *J. Am. Chem. Soc.* 125 (2003) 10402.
- [6] M.M. Ren, Z. Zhou, X.P. Gao, W.X. Peng, J.P. Wei, *J. Phys. Chem. C* 112 (2008) 5689.
- [7] H. Huang, T. Faulkner, J. Barker, M.Y. Saidi, *J. Power Sources* 189 (2009) 748.
- [8] M.Y. Saidi, J. Barker, H. Huang, G. Adamson, *Electrochem. Solid-State Lett.* 5 (2002) A149.
- [9] Y. Chen, Y.M. Zhao, X. An, J. Liu, Y. Dong, L. Chen, *Electrochim. Acta* 54 (2009) 5844.
- [10] X.H. Rui, C. Li, C.H. Chen, *Electrochim. Acta* 54 (2009) 3374.
- [11] J. Barker, M.Y. Saidi, J.L. Swoyer, *J. Electrochem. Soc.* 150 (2003) A684.
- [12] M. Higuchi, K. Katayama, Y. Azuma, M. Yukawa, M. Suhara, *J. Power Sources* 119–121 (2003) 258.
- [13] X.F. Guo, H. Zhan, Y.H. Zhou, *Solid State Ionics* 180 (2009) 386.
- [14] G. Yang, G. Wang, W.H. Hou, *J. Phys. Chem. B* 109 (2005) 11186.
- [15] K.S. Park, J.T. Sona, H.T. Chung, S.J. Kim, C.H. Lee, H.G. Kim, *Electrochem. Commun.* 5 (2003) 839.
- [16] G.T. Zhou, O. Palchik, V.G. Pol, E. Sominski, Y. Koltypin, A. Gedanken, *J. Mater. Chem.* 13 (2003) 2607.
- [17] G. Yang, Y. Kong, W.H. Hou, Q.J. Yan, *J. Phys. Chem. B* 109 (2005) 1371.
- [18] T.A. Nissinen, Y. Kiros, M. Gasik, M. Leskela, *Chem. Mater.* 15 (2003) 4974.
- [19] M. Nakayama, K. Watanabe, H. Ikuta, Y. Uchimoto, M. Wakihara, *Solid State Ionics* 164 (2003) 35.
- [20] A.C. Larson, R.B. Von Dreele, General Structure Analysis System (GSAS), Los Alamos National Laboratory Report LAUR, 2000, 86–748.